REGIONAL CEREBRAL BLOOD FLOW: A COMPARISON OF 8-DETECTOR AND 16-DETECTOR INSTRUMENTATION

O. B. Paulson, S. Cronqvist, J. Risberg and F. I. Jeppesen

Bispebjerg Hospital, Copenhagen, Denmark and University Hospital, Lund, Sweden

Measurement of the average blood flow in the human brain has been reported in numerous clinical studies. While immensely increasing our knowledge of the physiology and pathophysiology of the cerebral circulation, it has not given results of diagnostic clinical value. Recently the intra-arterial ^{133}Xe-injection technique for regional cerebral blood flow (rCBF) measurement has been applied to patient studies. With this technique such meaningful correlations have been found that clinical usefulness might well become a reality (*1,2*).

A crucial aspect of the rCBF technique is the resolution of the external gamma-ray detector. The rapid tissue clearance essentially prevents the use of conventional brain-scanning techniques. Even the gamma camera has limited possibilities because it has a finite deadtime. Therefore one cannot exploit the advantage of injecting the very large dose of radioactive gas which the very low radiation dose permits (*3*). Exploratory studies with an Anger camera have not yielded promising results (*4,5*). So far only multiple discrete channels have been useful. In this context the problem arises of how many probes can meaningfully be used; is better clinical information obtained with an increased number of probes?

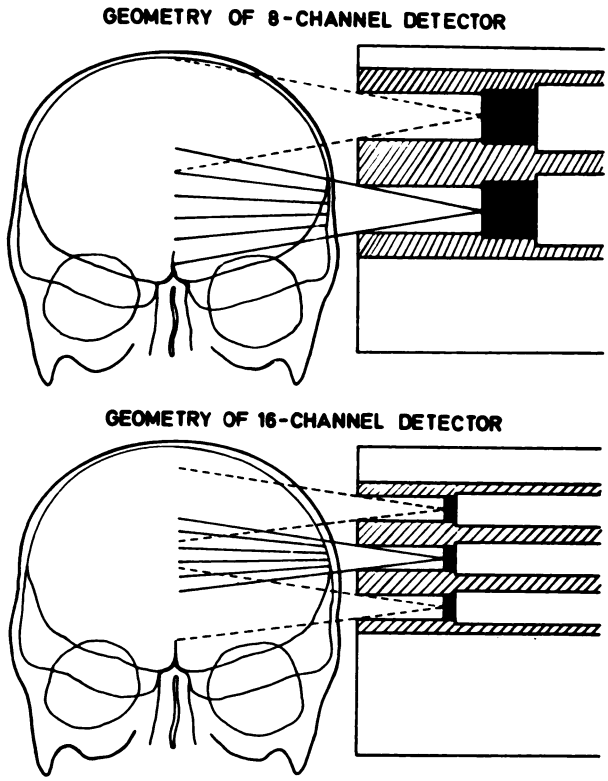

FIG. 1. Geometry, arrangement and counting areas for 8-detector and 16-detector instruments.

In this study one 8-detector and one 16-detector unit, developed and used in Lund and in Copenhagen, respectively, were compared by making repeated rCBF measurements in the same patient with focal cerebral disease. The 8-detector unit was used first and then the 16-detector unit (Figs. 1–3). In making the comparison, special emphasis was put on analysis of the first 2 min of the ^{133}Xe-clearance curves (Figs. 4, 5). This first part of the curve is of special interest in cases with tumors (*6*), arteriovenous malformations (*7*) and vascular lesions (*1*) as well as in studies of the effect of different pharmacological agents on cerebral blood flow (*1*).

MATERIALS AND METHODS

Ten patients were studied: six had supratentorial tumors (four had cerebral gliomas, one had a cerebral metastasis and one had a meningioma), one had an infratentorial tumor and three had cerebrovascular lesions. In the group of three with cerebrovascular lesions, one (Case 7) had transient ischemic attacks and the angiographic study showed a stenosis of the internal carotid artery, one (Case 9) had an apoplexy in which the angiographic study

Received June 4, 1968; revision accepted Sept. 20, 1968.

For reprints contact: O. B. Paulson, Dept. of Neurology, Bispebjerg Hospital, Copenhagen NV, Denmark.

showed an early filling vein and one (Case 10) had an intracerebral hematoma (see Table). The diagnoses were established by clinical history, angiography and, in some cases, pneumoencephalography. Diagnoses were verified by craniotomy in the six cases with supratentorial tumors and in the case with an intracerebral hematoma.

The regional blood-flow measurement is made by rapidly injecting ^{133}Xe dissolved in saline into the internal carotid artery and measuring the clearance with scintillation detectors (*8*). The 8-detector instrument (Nukab, Gothenberg, Sweden) consisted of 8 probes with 25.4 × 25.4-mm NaI(Tl) crystals collimated by 63-mm-long lead tubes (i.d., 23 mm) (Fig. 1). The 16-detector instrument (Meditronic, Copenhagen, Denmark) consisted of 16 probes with 11.5 × 5 mm NaI(Tl) crystals collimated by 43-mm-long lead tubes (i.d., 12 mm) (Fig. 1).

With both systems the probes were placed perpendicular to the saggital plane and lateral to the skull on the side of the hemisphere to be studied (Fig. 1). We assessed the position of the probes relative to the head by taping small pieces of lead on the head at the center of three probes and taking an x-ray film of the cranium. In this study only supratentorial structures were investigated, i.e. structures supplied predominantly by the internal carotid artery.

The tissue counted by one detector can be represented by the tissue-block inside the truncated cone through the center of the surface of the crystal and through the opening of the collimator (Fig. 1). In a phantom experiment (with water in the phantom and skull between the phantom and the collimator) it was shown that the tissue inside this truncated cone accounts for approximately 65% of the counts. Thus there was some degree of overlapping with both instruments in the medial part of the hemisphere between the neighboring regions studied. This overlapping was somewhat greater with the 16-detector unit than with the 8-detector unit (Fig. 1). The areas within the outer part of the hemisphere measured by the detectors 3 cm from the surface of the collimators have been defined for both units as the areas described by the circumference of the truncated cones at that distance (Fig. 2). The total area covered by all detectors was somewhat larger for the 8-detector than for the 16-detector instrument (Fig. 2).

The counting field of the detectors can also be represented by the isoresponse curves in water (Fig. 3) although isoresponse curves have the disadvantage that they only concern point sources and not the extended sources actually counted experimentally. The circular counting areas of the detectors estimated at 3 cm from the surface of the collimator (see the circles in Fig. 2) correspond approximately to the area inside the 50% level of the isoresponse curves. This is valid for both units if one sets 100% counting efficiency in the center of these areas.

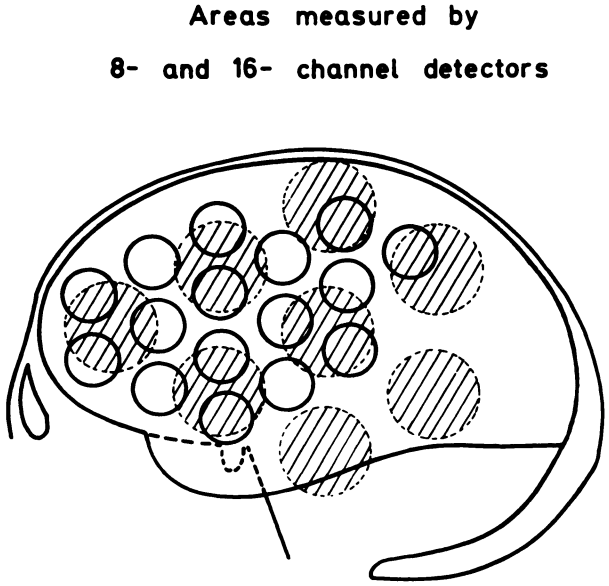

FIG. 2. Counting area of detectors 3 cm from collimator surface are shown. This corresponds to lateral part of hemisphere. Large circles represent 8-detector unit; small circles represent 16-detector unit. Figure shows that larger area of hemisphere is covered with 8-detector unit than with 16-detector unit.

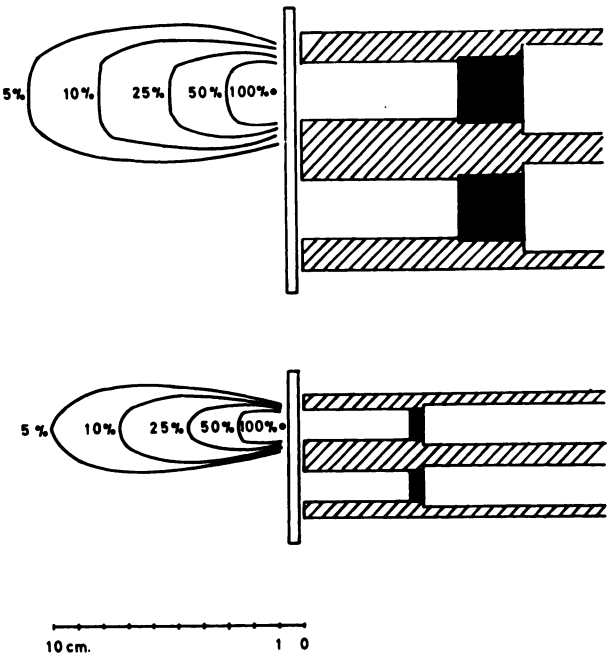

FIG. 3. Isoresponse curves in water for 8-detector and 16-dector units. 100% counting efficiency is set at 1 cm from surface of collimator.

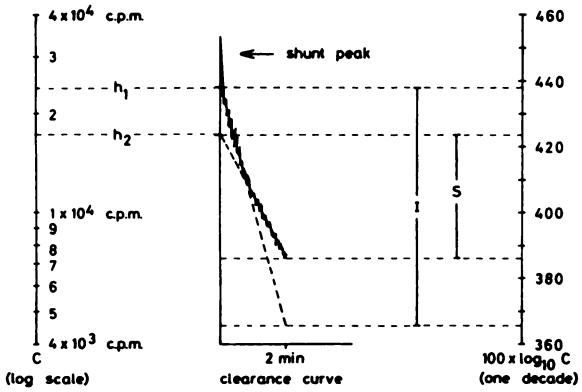

FIG. 4. Clearance curve with shunt peak and tissue peak, the latter being represented by bend in logarithmic clearance curve during first 2 min. Calculation of initial slope index (I), second minute slope index (S) and peak heights are shown. $I = 2D_{initial}$ and $S = 2D_{second\ min}$ (as I and S are measured over 2 min).

The 31-keV and 81-keV photopeaks of ^{133}Xe were counted using only lower-level discrimination at about 20 keV. The question of whether to count the 31-keV photopeak was evaluated experimentally. In phantom studies (with water in the phantom and skull between the phantom and the collimator) it was found that there is a decrease of only about 20% in efficiency when one raises the lower discrimination level from 20 to 50 keV. A significant increase in scatter measured as an increase in the percent of counts coming from areas outside the truncated cone could not be found. Using an even higher threshold decreases the Compton scatter, but results in a marked decrease in the counting rate, giving rise to poor counting statistics. Potchen *et al* have recently studied these problems. Calculating their figure of merit, one finds that a high threshold of 75 keV yields about the same figure as a low one of 20 keV while 50 keV actually gives the poorest value (9). The half-value layer in water was about 4.5 cm for the 81-keV photopeak and about 2.4 cm for the 31-keV photopeak. When counting both the 81 keV photopeak and the 31 keV photopeak, one obtains half activity under 4.2 cm of water. On the basis of the above evidence, it was decided to count both the 81-keV and 31-keV photopeaks.

Since the half value in water is about 4.2 cm, the depth resolution will be rather poor due to absorption of the gamma rays from the deeper structures. Therefore there will be a moderate over-representation of the superficial brain structures. Since the brain is an extended source of radiation, the inverse square law does not result in higher counting rate from superficial than from the deep layers.

With both units the pulses from each detector are recorded on a tape recorder. When the tape is replayed, the total number of counts (after 10 min) is registered on a scaler, and the counting rate is obtained with a ratemeter coupled to a recording potentiometer that has both linear and logarithmic recording. During the replay period the time constant of the ratemeter is 2 sec for the 8-detector system and 1 sec for the first 5 sec and 2 sec afterwards for the 16-detector system.

For the 8-detector unit 1 mCi of ^{133}Xe dissolved in 2-ml of saline was used, and a counting rate of approximately 75,000 cpm was reached in most channels. For the 16-detector unit 3 mCi of ^{133}Xe dissolved in 5–6 ml of saline was used, and a counting rate of approximately 25,000 cpm was reached in most channels. At this maximum counting rate the distortion of the clearance curves was negligible. The 8-detector unit had a loss of only 1% of the counts at a counting rate of 120,000 cpm and the 16-detector unit had a loss of only 2% at a counting rate of 300,000 cpm. The tape speed of the 8-detector unit was 3¾ in./sec, and all pulses were recorded (a de-randomizer was used). For the 16-detector unit, on the other hand, the speed of the tape was 7½ in./sec, and only every eighth pulse was recorded (no de-randomizing of the pulses was used).

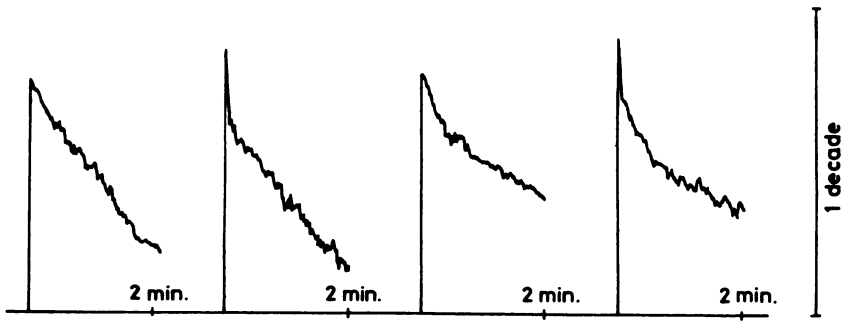

FIG. 5. Different configurations during first 2 min of clearance curves.

Calibration to equalize the gain of all detectors is not necessary because the gain does not affect the values calculated from the clearance curves (height of a curve divided by the area under it, slopes of a logarithmically recorded clearance curve and percent value of an intercept as described later). Only if one uses the height of a curve alone as a parameter is such a calibration necessary.

The isotope was injected into the internal carotid artery either through a needle after direct puncture of the vessel or through a catheter introduced from the femoral artery. The correct position of the needle or catheter was established by noting pallor in the medial part of the forehead after rapid injection of saline. In addition, the position was verified by angiography after the blood-flow study. The injection time was 1–1.5 sec. After each injection the syringe was allowed to fill with arterial blood to rinse the needle or catheter of remaining isotope solution before flushing with saline. After each isotope injection, an arterial blood sample was collected to determine the arterial pCO_2.

All cases were studied by serial angiography. The angiographic study was always performed after the rCBF study to avoid any influence on the cerebral blood flow by the contrast medium (*10*).

CALCULATIONS

Average 10-min flow value ($rCBF_{10}$). The average regional blood flow after 10-min clearance was calculated by the height/area method (*8*) as

$$rCBF_{10} = 100\lambda_a \frac{H_{10}}{A_{10}} \text{ ml/100 gm/min.} \quad (1)$$

100 is a factor for calculating flow/100-gm tissue. λ is the tissue-to-blood partition coefficient, and assuming a normal weight ratio of 60/40 between grey and white matter, the average ratio of λ (λ_a) has been used. In all cases the value 1.15 has been used for λ_a. H_{10} is the difference between the maximal counting rate—i.e. initial height—and the counting rate after 10 min of clearance—i.e. height after 10 min—both expressed in cpm. A_{10} indicates the area between the base line and the clearance curve followed for 10 min and is equivalent to the total number of counts measured during that time as registered by the scaler. The value of this area has to be corrected for background measured before isotope injection and also for remaining activity when isotope was previously injected (*8*).

Initial slope index (ISI—Fig. 4). In the first 2 min a cerebral clearance curve decreases almost monoexponentially in normal man (Fig. 5). When plotted on a logarithmic scale the slope of this first part of the curve gives an estimate of the cerebral blood flow within the region measured. Using this initial slope, a "flow value" can be calculated as (*1*)

$$rCBF_{initial} = 2.3\ \lambda_g\ D_{initial} \text{ ml/100 gm/min.}$$

The conversion factor from natural to logarithm to the base 10 is 2.3. Normally the clearance curve is dominated by the blood flow of the grey matter during the first 2 min (*8*). Therefore λ_g is the tissue-to-blood partition coefficient for grey matter which is about 0.87 (*8*). $D_{initial}$ is the initial slope of the curve in percent of decade per minute (not including the first 3–4 sec of the curve for reasons mentioned under "appearance of two first minutes of clearance curves.")

Because $2.3 \times 0.87 = 2.0$, the formula can be reduced to

$$rCBF_{initial} = 2D_{initial} \text{ ml/100 gm/min.}$$

However, because the value calculated in this manner is mathematically not actual flow but only an estimate of it and because we also want to use an analog value for the second minute (as mentioned below), we prefer to use the term initial slope index (ISI). Thus

$$ISI = 2D_{initial}. \quad (2)$$

It would have been possible to use only the slope $D_{initial}$ as the initial slope index. However, by using the factor 2 we arrive at an initial slope index number that is the same as the $rCBF_{initial}$ often used. The value obtained is about the same as that of the $rCBF_{10}$ as is mentioned later. We also avoid using decimals which might have been necessary if we had only used $D_{initial}$ as the slope index.

Second minute-slope index (SMSI—Fig. 4). Since the clearance curve over focal cerebral disease does not decrease monoexponentially in the first 2 min as stated below (Figs. 4 and 5), we have also used a second slope index—the second minute slope index (SMSI). This value is obtained in the same way as the initial slope index, but the first minute is neglected and only the slope of the clearance curve in the second minute is used.

The value is calculated as

$$SMSI = 2D_{second\ minute}. \quad (3)$$

Peak height (PH—Fig. 4). Another way to characterize an initial abnormality of a curve is to use the zero-time intercepts of the two components mentioned above. An index is calculated in the following way: the height (in cpm) of the zero-time intercept of the initial tangent is denoted h_1 and that of the tangent for the second minute h_2. Then

$$PH\ (\%) = \frac{h_1 - h_2}{h_2} 100 \quad (4)$$

TABLE 1. CORRELATION OF LOCATION OF FLOW ABNORMALITIES

Case no.	Age and sex	Diagnosis	Parameters*	Study with 8-detector (channel) unit: No. channels over lesion	Mean values over lesion	Mean values over non-lesion	No. channels with abnormal clearance curves†	No. channels with tissue peaks	Arterial pCO_2
1	M 27	Astrocytoma with malignant degeneration	$rCBF_{10}$	2	71	53	1	1	33
			ISI		86	61			
			SMSI		60	61			
			PH(%)		25	0			
2	M 63	Glioblastoma	$rCBF_{10}$	4	51	24	7	7	30
			ISI		312	85			
			SMSI		38	39			
			PH(%)		39	20			
3	M 50	Glioblastoma	$rCBF_{10}$	2	38	29	2‡	2	35
			ISI		74	51			
			SMSI		21	51	(+2)		
			PH(%)		19	0			
4	M 49	Glioblastoma	$rCBF_{10}$	2	23	26	1	1	44
			ISI		98	22			
			SMSI		17	22			
			PH(%)		28	0			
5	M 56	Metastasis	$rCBF_{10}$	1	38	29	2	2	33
			ISI		156	33			
			SMSI		31	28			
			PH(%)		85	4			
6	M 58	Infratentorial tumor	$rCBF_{10}$	0	—	40	0	0	37
			ISI		—	31			
			SMSI		—	31			
			PH(%)		—	0			
7	M 64	Transient ischemic attacks. Date of last attack not known.	$rCBF_{10}$	0	—	44	0	0	43
			ISI		—	46			
			SMSI		—	46			
			PH(%)		—	0			
8	F 40	Meningioma	$rCBF_{10}$	3	43	40	1	0	39
			ISI		43	38			
			SMSI		43	38			
			PH(%)		0	0			
9	M 81	Apoplexy. 2 days after acute attack	$rCBF_{10}$	2	16	17	1	1	30
			ISI		15	21			
			SMSI		15	16			
			PH(%)		0	4			
10	F 56	Intracerebral hematoma. 4 days after acute attack	$rCBF_{10}$	2	43	30	3	1	38
			ISI		54	41			
			SMSI		54	35			
			PH(%)		0	8			

* $rCBF_{10}$ = 10-min flow value; ISI = initial slope index; SMSI = second minute slope index; PH(%) = peak height in percent. Normal values: $rCBF_{10}$ = 50 ml/100 gm/min, ISI = SMSI = 55 and PH = 0%.

† These columns indicate focal abnormalities of flow in parts of the hemisphere, as distinct from generalized depression of flow.

WITH LESION SHOWN ANGIOGRAPHICALLY

Study with 16-detector (channel) unit					
No. channels over lesion	Mean values over lesion	Mean values over non-lesion	No. channels with abnormal clearance curves†	No. channels with tissue peaks	Arterial pCO_2
3	70	51	4	3	40
	104	49			
	51	49			
	37	0			
7	47	26	10	10	29
	131	64			
	25	20			
	104	18			
4	35	30	5	5	33
	62	35			
	29	27			
	20	6			
7	29	27	11	11	40
	73	47			
	21	23			
	22	10			
5	28	32	5‡	5	35
	38	45			
	26	35	(+5)		
	13	4			
0	—	30	0	0	37
	—	31			
	—	31			
	—	0			
0	—	37	1	0	45
	—	38			
	—	37			
	—	1			
4	43	38	5	3	39
	50	36			
	35	36			
	9	0			
1	15	16	1	1	29
	12	15			
	12	13			
	0	1			
3	35	32	6	3	35
	39	36			
	34	29			
	7	6			

‡ In these two cases additional adjacent channels showed clearance curves which were just at the limit of being abnormal (indicated by parentheses).

RESULTS

Appearance of two first minutes of clearance curves. In control cases (seven healthy young men) previously studied, we observed that the clearance curve decreased essentially monoexponentially for the first 2 min of clearance (Fig. 5). Only a few of the logarithmically plotted curves showed a small decrease of the slope in the last 15–20 sec of the first 2 min of clearance. This was usually seen in the curves with the highest flow values. Therefore the initial slope index and the second minute slope index in all these control cases showed the same value, and the peak heights were zero percent. The value of the initial slope index is normally about the same as or a little higher than the corresponding $rCBF_{10}$ values; for the control cases mentioned above the mean of the initial slope indices was 55, s.d. ±5.9, and of the $rCBF_{10}$ 50 ml/100 gm/min, s.d. ±5.4 ml/100 gm/min.

In the patients studied here, however, abnormal initial peaks were seen in one or more channels during the first minute of clearance indicating flow components faster than in the surrounding brain tissue. Two different types of peaks—the "arterial" or "shunt peak" and the "tissue peak"—were seen. In some cases both types of peaks appeared in a single clearance curve (Fig. 5).

The first type of peak—arterial peak or shunt peak (Fig. 5)—is very short; it lasts only 3–5 sec. Such a peak is normally encountered only over the carotid siphon, and it indicates a rapid passage of the entire bolus through the carotid artery to the hemisphere. Because it is never seen over the rest of the normal hemisphere, it cannot be due to overshoot of the graphic recorder. However, the same type of peak may also be encountered in other regions of the hemisphere in patients with arterio-venous malformations (7) or in rare cases of extremely vascular brain tumors (6). With the time constants used in our study—1 and 2 sec—the analysis of these very short shunt peaks is severely limited and only the more marked shunt peaks can be recognized. Therefore a detailed analysis of these peaks has not been made, and they are not included in the comparison of the 8-detector and 16-detector unit.

The second type of peak—tissue peak (Fig. 5)—varies in duration but always lasts several seconds and seldom exceeds 1 min. These peaks are represented by a bending during the first 2 min of the logarithmic recorded clearance curve, i.e. the first 2 min of the clearance curve is multiexponential rather than monoexponential. Peaks of this type indicate super-fast blood-flow components with rapid washout. They reflect hyperemia in brain or tumor tissue and have therefore been called tissue peaks. It is this

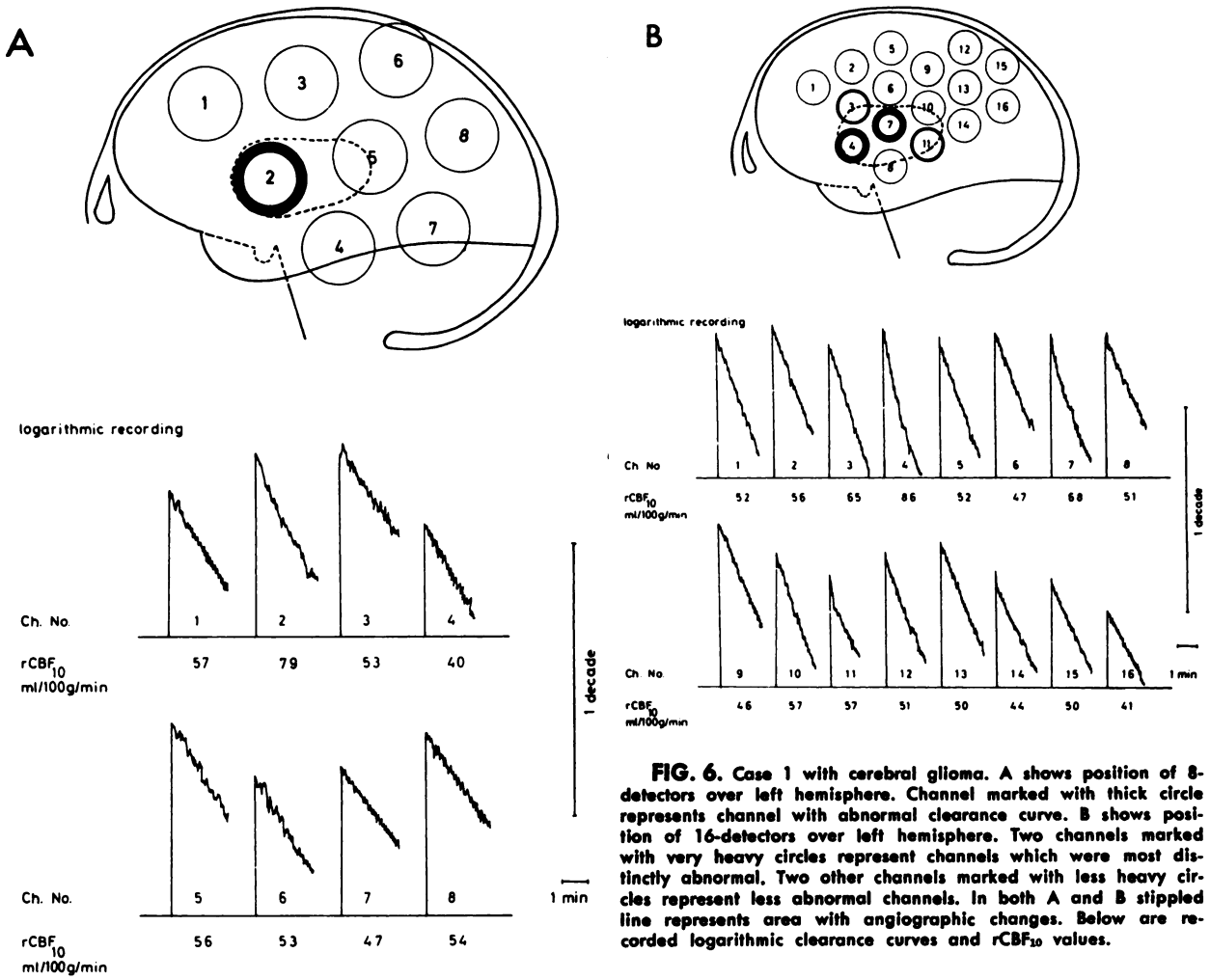

FIG. 6. Case 1 with cerebral glioma. A shows position of 8-detectors over left hemisphere. Channel marked with thick circle represents channel with abnormal clearance curve. B shows position of 16-detectors over left hemisphere. Two channels marked with very heavy circles represent channels which were most distinctly abnormal. Two other channels marked with less heavy circles represent less abnormal channels. In both A and B stippled line represents area with angiographic changes. Below are recorded logarithmic clearance curves and $rCBF_{10}$ values.

type of peak that is responsible for high values of the initial slope index and for the difference between the initial slope index and the second minute slope index. The peak height indicates the approximate percent of the bolus perfusing the hyperemic tissue (Fig. 4). Only a peak height larger than 10% was considered significantly abnormal.

In all cases in which abnormal $rCBF_{10}$ values were encountered, abnormalities were also seen in the first 2 min of the clearance curves in the form of a tissue peak or only an abnormal initial slope index. In three cases (Cases 3, 4 and 5) only the analysis of the first 2 min of clearance curve showed focal abnormalities. In each of these three cases tissue peaks were present, but the $rCBF_{10}$ values showed no regional abnormalities.

Comparison of 8- and 16-detector instruments. One of the 10 patients studied (Case 6) had no focal abnormalities of rCBF while the other nine patients had various focal abnormalities. In eight of these nine cases the abnormalities were seen with both the 8-detector and 16-detector systems. But in the remaining one (Case 7) the focal abnormalities were only seen with the 16-detector system (see Table). Using the 16-detector system in this case, one channel showed a tissue peak and high flow value (initial slope index 51, second minute slope index 33, peak height 16% and $rCBF_{10}$ 43 ml/100 gm/min). The values for the remaining part of the brain were: average initial slope index 36 and average $rCBF_{10}$ 32 ml/100 gm/min.

Twenty abnormal curves (of which 15 had tissue peaks) were found with the 8-detector unit and 53 (of which 42 had tissue peaks) were found with the 16-detector unit (see Table). The 16-detector unit had better resolution in practically all cases. Two of them are described below in detail:

Case 1. (Fig. 6A and B). The patient was a 27-year-old man who for the last half year had had increasing attacks of temporal lobe epilepsy. The angiographic study showed an expansive process in the left temporal region and abnormal vessels through which the contrast media passed rapidly. A subsequent operation revealed a temporal lobe astrocytoma with malignant degeneration.

With the 8-detector system (Fig. 6A) one channel corresponding to the focus showed an abnormal clearance curve (Channel 2). In this channel a tis-

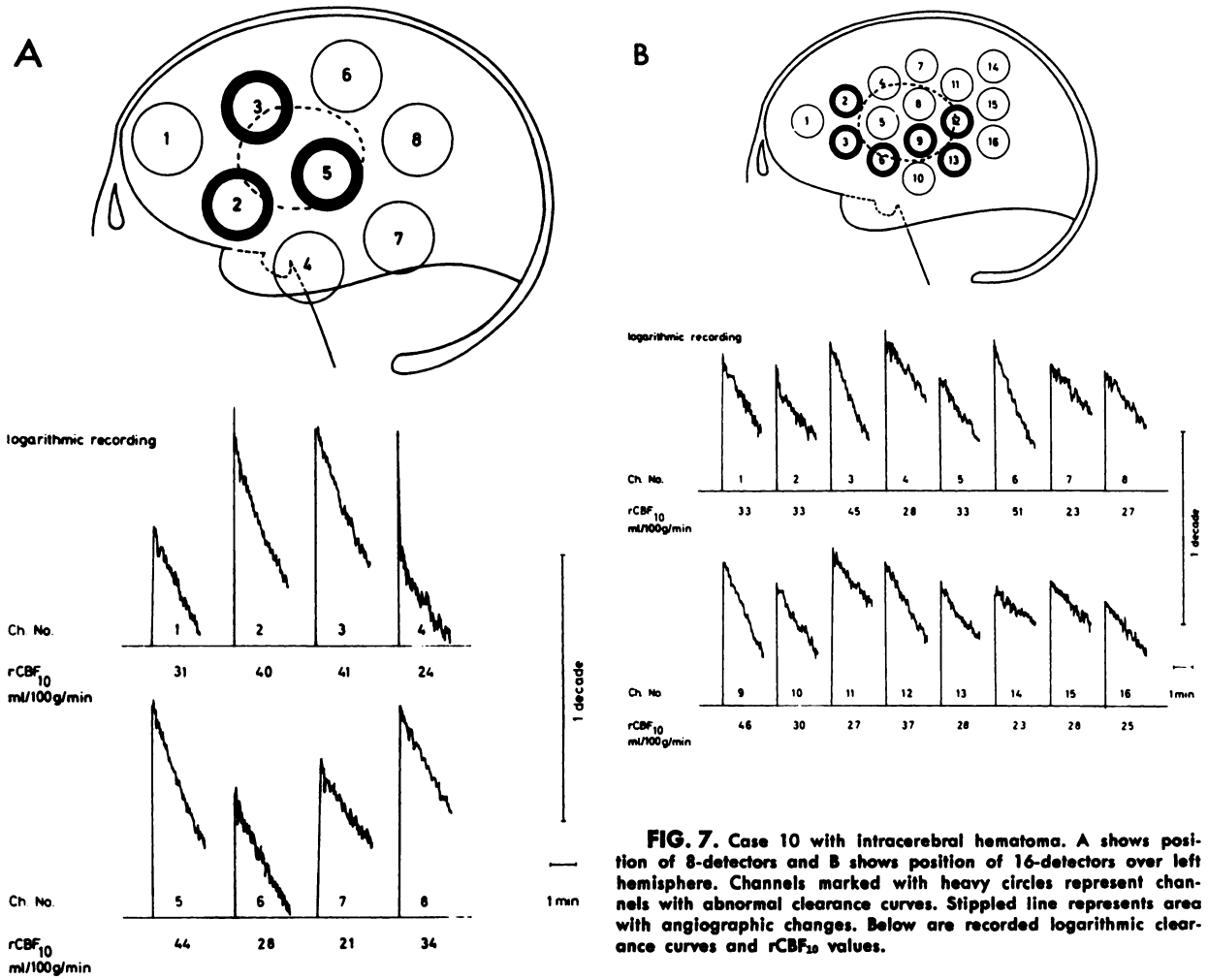

FIG. 7. Case 10 with intracerebral hematoma. A shows position of 8-detectors and B shows position of 16-detectors over left hemisphere. Channels marked with heavy circles represent channels with abnormal clearance curves. Stippled line represents area with angiographic changes. Below are recorded logarithmic clearance curves and $rCBF_{10}$ values.

sue peak was present (peak height 49%, initial slope index 109 and second minute slope index 57), and the $rCBF_{10}$ value was abnormally high (83 ml/100 gm/min). The values for the remaining "nonfocal" parts of the brain were all normal.

With the 16-detector system (Fig. 6B) four channels corresponding to the focus showed abnormal clearance curves (Channels 3, 4, 7 and 11). Two of these channels (Channels 4 and 7) were more distinctly abnormal than the others. In these two channels tissue peaks were present (peak heights 56% and 39%, initial slope indices 110 and 82 and second minute slope indices 60 and 46) and the $rCBF_{10}$ values were abnormally high (86 and 68 ml/100 gm/min). Channels 3 and 11 were less abnormal: in channel 3 no time peak was present but the $rCBF_{10}$ value was abnormally high (65 ml/100 gm/min), and the initial slope index was also high (63). In Channel 11 a tissue peak was present (peak height 17%, initial slope index 120, second minute slope index 56), but here the $rCBF_{10}$ value was normal (57 ml/100 gm/min). The values for the remaining nonfocal parts of the brain were all normal.

Case 10. (Fig. 7A and B). The patient was a 56-year-old female with hypertension of some years duration. Four days before the rCBF study she suddenly developed a right hemiparesis and aphasia. The angiographic study showed an avascular space-occupying lesion in the left frontoparietal region, and on the inferoposterior boundary of this lesion some early-filling veins were seen. At subsequent operation, a frontoparietal intracerebral hematoma about 5 cm in diameter was found.

With the 8-detector system (Fig. 7A) three adjacent channels over the region of the hematoma determined angiographically showed abnormalities. In these three channels (Channels 2, 3 and 5) the initial slope indices were 74, 53 and 54, the second minute slope indices 38, 53 and 54, the peak height 46%, 0% and 0% and the $rCBF_{10}$ values were 40, 41 and 44 ml/100 gm/min, respectively. The values for the remaining nonfocal parts of the brain were: average initial slope index 34 and average $rCBF_{10}$ 28 ml/100 gm/min.

With the 16-detector unit (Fig. 7B), however, it was possible to show that the areas with focally abnormal flow were at positions corresponding to

the lower boundary of the hematoma and not to the whole region of the hematoma. Six channels over this lower boundary zone showed abnormal clearance curves. In these six channels (Channels 2, 3, 6, 9, 12 and 13) the initial slope indices were 74, 52, 67, 52, 37 and 36, the second minute slope indices were 26, 52, 37, 52, 37 and 20, the peak heights were 18%, 0%, 44%, 0%, 0% and 16% and the $rCBF_{10}$ values were 33, 45, 51, 46, 37 and 28 ml/100 gm/min, respectively. The values for the remaining nonfocal parts of the brain were average initial slope index 26 and average $rCBF_{10}$ 28 ml/100 gm/min.

Correlation of location of flow abnormalities with angiographic changes. The angiogram was normal in one case which also lacked abnormalities of blood flow (Case 6; for clinical data see Table).

Focal angiographic changes were seen in 8 of the 9 remaining cases, and in the last one there was a stenosis of the internal carotid artery. The average flow values of the probes over the focal angiographic changes and over the rest of the brain were calculated (see Table). The average flow values of the 8-detector system were almost the same as those obtained with the 16-detector system. However, the value of this comparison is limited by the fact that two types of abnormalities (of anatomy and of tissue circulation) are seemingly not always coexistent. This is particularly clear in Case 10 in which flow abnormalities were only present around the space occupying avascular lesion (a hematoma) (Fig. 7B).

This limited degree of correlation between the two types of studies is theoretically not too surprising because anatomically normal brain tissue could well have circulatory alternations (*11*).

DISCUSSION

The present series includes only patients with clinical evidence of focal cerebral disease. This selection of cases was made purposely because the aim was to study the resolution of the 8-detector and 16-detector systems. Therefore from this series we cannot give data for the interchannel coefficient of variation in nonfocal cases. However, previous experience has indicated that the 8-detector unit has an interchannel coefficient of variation of 7% (*12*) while the 16-detector unit has an interchannel coefficient of variation of 9% (*1*). Both coefficients have a standard deviation of about 3%, i.e., the observation of a coefficient of variation exceeding 15% may be regarded as abnormal with some confidence. In the present series one of the ten patients (Case 6, see Table) showed no regional abnormalities of blood flow. The interchannel coefficient of variation was 11% with both the 8-detector and the 16-detector unit in this case.

When comparing the coefficients of variation, it should be remembered that the counting rate of the 8-detector system was about three times higher than that of the 16-detector system. The resulting difference in counting statistics, however, is not reflected in differences in the interchannel coefficient of variation. Even the difference in counting geometry does not appear to influence this variation significantly. Since the radiation exposure is exceedingly low (*3*), one could increase the dose of radioactivity considerably and therefore use even smaller crystals and counting regions without making the counting rate in each channel too low. But by using smaller crystals and counting regions in an attempt to obtain higher resolution, the differences in counting geometry would possibly influence the coefficient of variation markedly. In the smaller counting regions there could be a larger physiological variation of the regional cerebral blood flow due to a variable amount of grey matter and other nonhomogeneities in the brain. But so far this limiting degree of resolution has apparently not been found.

In the nine cases with focal abnormalities, the abnormalities were seen only in eight of them using the 8-detector unit, but in all of them using the 16-detector system. Furthermore, with the 16-detector system much better resolution and therefore better localization of brain tissue with disturbed circulation was obtained. This is most clearly seen in the case with an intracerebral hematoma (Case 10) where the 16 small detectors but not the 8 larger ones showed that the tissue with abnormal flow values was located in the region of the lower boundary of the avascular hematoma (Fig. 7A and B). Since the avascular space occupied by the hematoma receives no blood and therefore no isotope, it does not contribute to the shape of the clearance curves.

If routine clinical use of regional CBF studies eventually becomes a reality, the smallest number of probes giving adequate resolution should obviously be used. But at present we have no knowledge of the maximum obtainable resolution nor of the clinically useful level of resolution, and all that can be said from analogy with x-ray photography is that clinical diagnostic work can usually use all the resolution possible.

The results showed that no information was lost when we analyzed only the first 2 min of the clearance curve. In fact, analyzing this part of the curve gives information in addition to that obtained from the $rCBF_{10}$ value. This means that the problems of data processing may be reduced considerably if one uses only the shape of the first 2 min of the clear-

ance curve when plotted logarithmically, instead of following the clearance curve for 10 min.

In concluding, the following comments can be made about the future development of instrumentation for measuring regional cerebral blood flow. The use of more probes poses the problem of how to process the many clearance events more rapidly and efficiently. The use of a multitrack tape recorder replaying simultaneously through several ratemeters is highly impractical. A faster playback is offered by using a magnetic core memory instead of tape (*13*). The instantaneous record provided by having a ratemeter on each channel and displaying its output simultaneously on an oscilloscope screen seen by a Polaroid camera allows one to obtain all the curves almost immediately (*14*). As mentioned in the introduction, gamma-camera techniques are also being applied to regional inert gas clearance from the human brain (*4,5*). The most logical approach would be the development of a gamma camera with zero deadtime, which would allow simultaneous recording of many pulses. However, digital information would have to be used. But until such an instrument is developed, independent detectors are the only means of effectively reducing the over-all deadtime of the instrument. The zero deadtime is of course necessary if one is to use larger doses of radioactivity which yield a total of several millions of counts per minute. The safety of these larger doses of radioactive inert gases has been well defined (*3*).

SUMMARY

An 8-detector and a 16-detector system for measuring regional cerebral blood flow (rCBF) using a slug injection of ^{133}Xe into the internal carotid artery have been compared in a group of ten patients with focal cerebral disease.

The results have been analyzed with special regard to the abnormalities encountered in the first two minutes of the clearance curves. These abnormalities are described in detail (shunt peak, tissue peak, abnormal initial slope index). The 10-min flow values ($rCBF_{10}$) have also been calculated but were found to give less information than the analysis of the first 2 min of the clearance curves.

Focal abnormalities were found with greater frequency and much better resolution, and more detailed information was obtained using the 16-detector instrument.

ACKNOWLEDGMENT

This study was supported by grants from Riksföreningen mot Cancer, Stockholm, Sweden, the Swedish Medical Research Council, B 67-21x-84-03, and the Wallenberg Foundation, Stockholm, Sweden.

The authors are indebted to N. A. Lassen, Bispebjerg Hospital, Dept. of Clinical Physiology, Copenhagen, Denmark, to D. H. Ingvar, University Hospital, Dept. of Neurophysiology, Lund, Sweden, and to E. Skinhøj, Bispebjerg Hospital, Dept. of Neuromedicine, Copenhagen, Denmark, for their valuable help.

REFERENCES

1. Høedt-Rasmussen, K., Skinhøj, E., Paulson, O., Ewald, J., Bjerrum, J. K., Fahrenkrug, A. and Lassen, N. A.: Regional cerebral blood flow in acute apoplexy. The "luxury perfusion syndrome" of brain tissue. *Arch. Neurol.* **17**:271, 1967.

2. Cronqvist, S. and Laroche, F.: Transitory hyperemia in focal cerebral vascular lesions studied by angiography and regional cerebral blood flow measurement. *Brit. J. Radiol.* **40**:270, 1967.

3. Lassen, N. A.: Assessment of tissue radiation dose in clinical use of radioactive inert gases, with examples of absorbed doses from H_2^3, Kr^{85} and Xe^{133}. In *Radioaktive Isotope in Klinik und Forschung,* vol. 6, ed. Fellinger, K. and Höfer, R. Urban & Schwarzenberg, München & Berlin, 1965, p. 37.

4. Loken, M. K., Pierce, R., Resch, J., Lassen, N. A. and Ingvar, D. H.: Regional circulation in the brain using a scintillation (Anger) camera. *Minn. Med.* **50**:497, 1967.

5. Rosenthall, L., Mathews, G. and Stratford, J.: Radio-xenon brain scanning with the gamma-ray scintillation camera. *Radiology* **89**:324, 1967.

6. Cronqvist, S., Ingvar, D. H. and Lassen, N. A.: Quantitative measurements of regional cerebral blood flow related to neuroradiological findings. *Acta Radiol.* **5**:760, 1966.

7. Häggendal, E., Ingvar, D. H., Lassen, N. A., Nilsson, N. J. P., Norlén, G., Wickbom, A. and Zwetnow, N.: Pre- and postoperative measurements of regional cerebral blood flow in three cases of intracranial arteriovenous aneurysm. *J. Neurosurg.* **22**:1, 1965.

8. Høedt-Rasmussen, K., Sveinsdottir, E. and Lassen, N. A. Regional cerebral blood flow in man determined by intra-arterial injection of radioactive inert gas. *Circulation Res.* **18**:237, 1966.

9. Potchen, E. J., Davis, D. O., Wharton, T., Clifton, J.: The effect of Compton scatter on regional cerebral blood flow determinations with xenon-133. *Clin. Res.* **15**: 410, 1967.

10. Cronqvist, S.: Regional cerebral blood flow and angiographic findings in 61 cases with cerebrovascular disorders. *Acta Radiol.* In press.

11. Cronqvist, S. and Agee, F.: Regional cerebral blood flow in intracranial tumours. *Acta Radiol.* **7**:393, 1968.

12. Ingvar, D. H., Cronqvist, S., Ekberg, R., Risberg, J. and Høedt-Rasmussen, K.: Normal values of regional cerebral blood flow in man, including flow and weight estimates of gray and white matter. *Acta Neurol. Scand.* Suppl. **14**:72, 1965.

13. Risberg, J., Ingvar, D. H., Lundmark, T., von Sabsay, E., Burklint, U. and Sundelin, S.: Recording of multiple clearance curves by means of a magnetic core memory. *Scand. J. Clin. Lab. Invest.* Suppl. **22**:102, XI:H, 1968.

14. Lassen, N. A.: Preliminary experience with oscilloscope and Polaroid camera as recorded unit in a multichannel scintillation detector instrument. *Scand. J. Clin. Lab. Invest.* Suppl. **22**:102, XI:I, 1968.